Astron. Astrophys. 340, 216–221 (1998)

ASTRONOMY AND ASTROPHYSICS

A BeppoSAX/LECS X-ray observation of α Centauri

R. Mewe[1], **M. Güdel**[2], **F. Favata**[3], **and J.S. Kaastra**[1]

[1] Space Research Organization Netherlands (SRON), Sorbonnelaan 2, 3584 CA Utrecht, The Netherlands
[2] Paul Scherrer Institut, Würenlingen und Villigen, CH-5232 Villigen PSI, Switzerland
[3] Astrophysics Division - Space Science Department of ESA, ESTEC, Postbus 299, 2200 AG Noordwijk, The Netherlands

Received 16 July 1998 / Accepted 15 September 1998

Abstract. We present the X-ray spectrum of the nearby binary α Cen AB (G2V + K1V) that has been obtained from observations with the low-energy concentrator (LECS) onboard the BeppoSAX X-ray astronomy satellite. SAX combines, in contrast to previous satellites, simultaneous coverage of the 0.1-10 keV energy range with sufficient spectral resolution to determine emission measure distributions and elemental abundances of soft coronal sources. The analysis of the spectrum using the SPEX plasma emission code shows a two-temperature structure of the corona which is confirmed by a differential emission measure analysis. It reveals a soft ($\sim$ 0.1 keV) component as detected previously by EUVE and ROSAT and a hard ($\sim$ 0.5 keV) component comparable to that seen by EINSTEIN, EUVE, and ASCA. The derived coronal Fe abundance of 0.7 ± 0.3 (relative to solar photospheric) is consistent with the solar photospheric abundance but marginally (3σ) different from the value of the metal-rich photosphere of α Cen. The abundance ratios Mg/Fe and Si/Fe are consistent (within 1σ) with solar photospheric and coronal values, whereas the O/Fe ratio ($3\pm$ 2) appears too high but the uncertainty is large. The X-ray flux in the 0.1-2.4 keV band is comparable to the average of previous observations with other instruments and to that derived from the ASCA observations if the different passbands of the instruments are taken into account. The two-temperature structure is reminiscent of recently determined emission measure distributions of the solar corona; the hotter component may be evidence for flare heating.

Key words: stars: abundances – stars: activity – stars: coronae – stars: individual: α Cen – stars: late type – X-rays: stars

1. Introduction

α Cen A is a close twin to the Sun, showing coronal properties that are very reminiscent of the properties of the solar corona. It is a member of the binary system α Cen AB (HD 128620/1) that lies at a distance of 1.34 pc from the Sun and consists of a $1.1M_\odot$ G2 V star with a radius of $1.24R_\odot$ and a $0.9M_\odot$ K1 V star with a radius of $0.84R_\odot$ (e.g., Flannery & Ayres 1978; for further details we refer to Paper II).

Send offprint requests to: R. Mewe, (R.Mewe@sron.nl)

In two previous papers Mewe et al. (1995a, 1998, hereafter referred to as Papers I and II, respectively) have discussed the coronal temperature structure and X-ray flux as determined from observations with other instruments (EUVE, EINSTEIN, ROSAT, and ASCA). In Paper II we discussed the coronal abundances as derived from EUVE and ASCA and found that there are indications that these may differ from the corresponding solar photospheric values as given by Anders & Grevesse (1989). It is therefore important to measure the abundances also with BeppoSAX which has the advantage (over ROSAT and ASCA) of combining the soft energy range of ROSAT with the hard energy range of ASCA . It thus covers the full energy range from 0.1 up to about 10 keV needed to interpret the coronal temperature structure with the necessary spectral resolution to reconstruct emission measure distributions and to derive abundances.

In the present paper, we derive the coronal temperature structure and elemental abundances from data observed with the LECS and compare these with the results from ASCA and from other instruments.

2. Observations and data reduction

The source α Cen was observed in 1997 from February 23 07:22 UT to February 24 07:59 UT with the low-energy concentrator (LECS; 0.1–10 keV) and medium-energy concentrator (MECS; 1.3–10 keV) spectrometers onboard the BeppoSAX X-ray astronomy satellite. For a description of the LECS and MECS instruments we refer to Parmar et al. (1997) and Boella et al. (1997), respectively. During the period of the observations the light curves did not show any significant time variability.

Although the net observation time of the MECS (49 ks) was larger than that of the LECS (26 ks) we have used the MECS spectrum only for checking the LECS results because the source spectrum is very soft and declines steeply, being below the background level in most of the MECS energy range (i.e. $\gtrsim$ 2 keV). The MECS data were reduced using an extraction radius of 4′.

The LECS data were reduced through the LECS pipeline software (SAX-LEDAS v.1.4.0), the extraction of the source and background spectra was done within the FTOOLS/XSELECT package, and the response matrix was pro-

duced with the LEMAT v.3.2.0 software. The source spectrum was extracted from a circle with a radius of 35 pixels (corresponding to 8′) which allows 95% of the source counts at 1 keV to be included. The source spectrum was rebinned to ensure a sufficient signal–to–noise ratio S/N per bin, i.e. S/N $\gtrsim$ 2 corresponding to $\gtrsim$ 10 counts per rebinned channel. Bins with energies below $\sim$ 0.1 keV and above $\sim$ 1.5 keV were discarded. This yields a spectrum of 18 bins between 0.092-1.55 keV. The background was derived from long observations of empty fields, and was extracted from the same detector area as the source. The resulting source count rate is 0.090 cts/s, to be compared with a background rate (for the same region and spectral interval), of 0.0054 cts/s. The background-subtracted LECS spectrum is shown in Fig. 1, together with the best-fit two-temperature model discussed in Sect. 4.1.

3. Spectral fitting

For the rebinning of the spectrum, the background subtraction, and the spectral analysis, we have used the SPEX v.1.10 software package (Kaastra et al. 1996a). This package contains models for the calculation of spectra from optically thin plasmas in collisional ionization equilibrium (CIE) (Mewe et al. 1985, 1986; Kaastra & Mewe 1993). The calculations for the Fe-L complexes have been updated using results from the HULLAC code (Liedahl et al. 1995b) and various other improvements have been made resulting in the MEKAL code (cf. Mewe, Kaastra, and Liedahl 1995b). We express abundances relative to the solar photospheric values taken from Anders & Grevesse (1989) (AG89). For the ionization balance we use Arnaud & Rothenflug (1985) for all elements except iron, for which we use the update of Arnaud & Raymond (1992). Emission measures are defined here as $EM = \int n_{\rm e} n_{\rm H} {\rm d}V$, where $n_{\rm e}$ is the electron density, $n_{\rm H}$ is the hydrogen density and V the emitting plasma volume.

We note that no assumption has been made concerning the geometry of the emitting plasma structure. By definition we determine the emission measure on the visible hemisphere on the star from the observed flux, with no inference about the emission measure distribution on the other hemisphere. Therefore, our luminosity values are representative for the observed emission measure. So we do not make any correction, e.g., by muliplying EM by a factor of two as sometimes authors do assuming that only half of the coronal photons are seen. However, this is only true for the special case of a homogeneous atmosphere close to the star.

Galactic absorption is taken into account using the model of Morrison & McCammon (1983). As a check of the results obtained using SPEX, we have repeated some of the spectral analysis using the independent spectral analysis package XSPEC v.9.0. We obtained essentially the same results using XSPEC as with SPEX, so we will not discuss the XSPEC spectral analysis.

3.1. Differential emission measure (DEM) modeling

For a multi-temperature plasma we introduce the differential emission measure $D(T) = n_{\rm e}(T) n_{\rm H}(T) dV/d\log T$. This is the weighting function that describes the contribution by the plasma, at each temperature T, to the observed spectrum. To derive physical parameters from the spectra various techniques can be applied. As an extension to the usual multi-temperature fitting technique using δ-functions (cf. Sect. 4.1.), we can apply a DEM analysis method which uses other basic functions. For example, in the present paper we use the Gauss fitting method. The basic functions are Gaussian functions of log$T$ with a finite temperature width (characterized by the "standard deviation" σ in log$T$, where 2.35$\times\sigma$ is the FWHM). We further use a genetic algorithm that is based on the biological notion of evolution by means of natural selection. By breeding an initial population of randomly chosen solutions with an assigned "fitness", using crossover and mutation of the genes of the individuals, the population gradually evolves towards a solution of higher fitness. For a detailed description of all DEM analysis techniques implemented in SPEX we refer to Kaastra et al. (1996b) and also to Mewe et al. (1996a,b). We display the results as the emission measure integrated over a temperature bin, i.e. $DEM = D(T)\Delta \log T$ so that the total emission measure within a certain temperature range follows by summing the values of DEM for the relevant temperature bins.

4. Results

Because the fits are not sensitively dependent on the interstellar hydrogen column density we used a fixed value of $N_{\rm H} = 10^{18}$ cm^{-2} which is approximately equal to the best-fit value obtained in the analysis of the EUVE spectrum of α Cen (Paper I) .

4.1. Temperature and abundance analysis

We first attempted to fit the spectrum with one- and two-temperature models using the solar photospheric abundances as given by AG89 (see also Paper II). We obtained very poor fits with minimum χ^2 = 346 and 24 (16 and 14 d.o.f.), respectively, showing that even a two-temperature fit is not sufficient. The experience for other coronal sources shows that the fit can improve considerably if the abundances are left free to vary. Simulations by Favata et al. (1998) for a two-temperature (0.5 & 2 keV) model with varying abundances show that for 10^4 accumulated counts per spectrum (note that α Cen has only 2225 cts) the LECS can constrain only a few abundances: Fe within about 15-25% (1σ), and O, Mg, and Si within from $\sim$ 30% up to $\sim$ 50%, respectively, while other abundances (e.g., S and Ne) are much less constrained. By varying these four abundances the fit is considerably improved: χ^2 = 9.3 for 10 d.o.f. with best-fit values for the temperatures (in keV) T_1 = 0.088 $\pm$ 0.013 and T_2 = 0.52 $\pm$ 0.08, and the emission measures (in 10^{49} cm^{-3}) EM_1 = 15 $\pm$ 4 and EM_2 = 2.4 $\pm$ 0.8. Adding of more temperature components does not further improve the fit. We experimented with fitting additional abundances but found that none of them

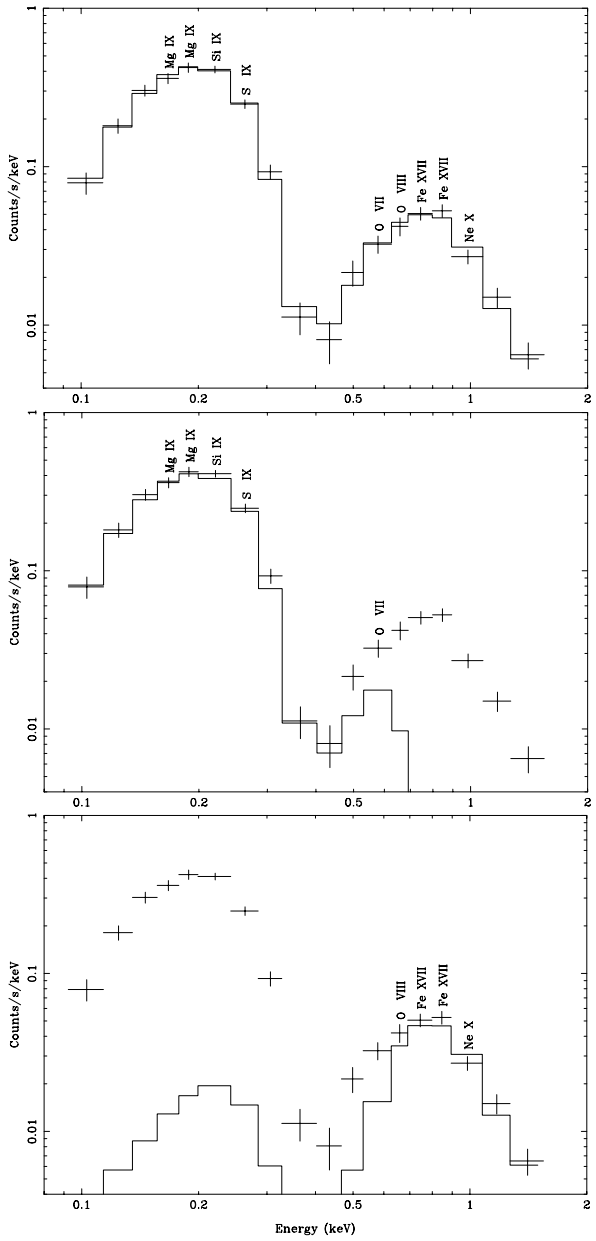

Fig. 1. Observed and best-fit two-temperature model (bold solid line) SAX LECS spectrum of α Cen, corrected for background (top panel). Error bars indicate $\pm 1\sigma$ errors of the observations. The positions of prominent lines containing more than 10 counts as predicted by the best-fit model are indicated by the ions from which they originate. The middle and the bottom panels show the contributions from the soft ($\sim$ 0.1 keV) and the hard (0.5 keV) component, respectively.

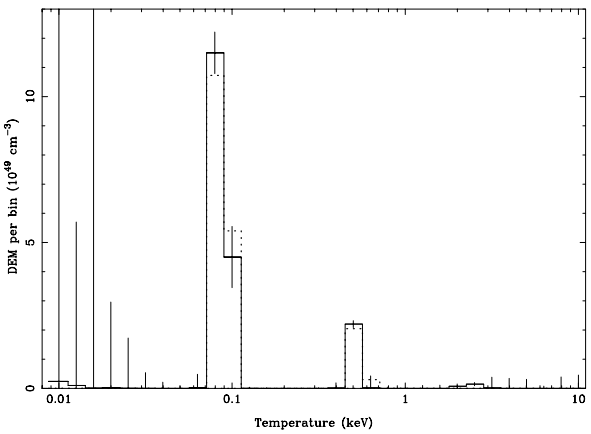

Fig. 2. The DEM (emission measure per temperature bin) as derived for the SAX LECS spectrum using the Multi-Gauss method with two temperature components and with the best-fit abundances (dotted line). For comparison the thin solid line with error bars gives the result of a genetic algorithm.

(viz., Ne, S, Ar, Ca, and Ni) were reasonably constrained. We have therefore assumed values of unity for these abundances.

The X-ray flux L_X (in units of 10^{27} erg/s) in the 0.1–2.4 keV energy interval is 3.48 with 80% coming from the soft ($\sim$ 0.1 keV) component and 20% from the 0.5 keV component.

For the abundances with respect to the corresponding solar photospheric values of AG89 we obtain: Fe: $0.67^{+0.33}_{-0.24}$; O: $2.2^{+1.8}_{-1.4}$; Mg: $1.2^{+1.0}_{-0.7}$; Si: $0.5^{+0.4}_{-0.3}$. By fixing the Fe abundance to its best-fit value of 0.67 and varying the other abundances we have determined the uncertainties in the ratios to the Fe abundance. The abundance ratios relative to Fe with respect to the corresponding solar photospheric abundance ratios are given in Table 1.

In previous work we have always taken as a standard reference the AG89 solar photospheric abundances. If we use the updated recommended (slightly lower) values given by Grevesse et al. (1992) (GNS92) for Fe (7.51) and O (8.87) we obtain: Fe: $0.95^{+0.48}_{-0.34}$ and O: $2.3^{+1.9}_{-1.2}$, and for the ratios [O/Fe] = $2.5\ ^{+2.0}_{-1.2}$, [Mg/Fe] = 1.3 ± 0.8, and [Si/Fe] = 0.5 ± 0.3. On the other hand, the photospheric abundances for α Cen are a little higher than the AG89 values (footnote 1 of Table 1).

We note that the given uncertainties are lower limits because of possible effects of systematic errors in the atomic data (excitation rates and ionization balance).

We have checked the results from the LECS by fitting the LECS spectrum combined with the small part (1–2.2 keV) of the MECS spectrum that is well above the background. It turns out that we have to multiply the LECS area by a cross-calibration factor of 0.715 in order to reconcile the LECS with the MECS. The results for the temperatures and abundances, and for the emission measures and flux (appropriately rescaled by the cross-calibration factor) were the same within the statistical uncertainties.

4.2. DEM analysis

In reconstructing the DEM we have applied the multi-temperature Gauss fitting method (cf. Sect. 3.1.).

We use a temperature grid between 0.01–10 keV with $\Delta \log T$=0.1 and adopt the set of best-fit abundances given in Sect. 4.1. We obtain χ^2 = 10 (12 d.o.f.) for two narrow Gaussian temperature components at 0.088 keV (σ = 0.004) and 0.54 keV (σ = 0.02) with emission measures of 16 10^{49} cm^{-3} and 2.3 10^{49} cm^{-3}, respectively (cf. dotted curve in Fig. 2). This confirms

Table 1. Abundance ratios for the corona of α Cen relative to the corresponding solar photospheric abundance ratios of Anders & Grevesse (1989)[1] as derived from SAX & ASCA observations and compared with corresponding values adopted for the average solar corona

	Abundance ratio		
	SAX[2]	ASCA[3]	Solar Corona[4]
[O/Fe]	$3.2^{+2.6}_{-1.6}$	0.3±0.14	0.34
[Mg/Fe]	1.9±1.1	4.4±1.0	1.4
[Si/Fe]	0.7±0.5	5.8±4.2	1.3

[1] Abundance values in logarithmic units, with $\log_{10}$H=12.00: O, 8.93; Mg, 7.58; Si, 7.55; Fe, 7.67; these values are a little (0.2 dex, for Fe 0.04 dex) smaller than the abundances adopted by Drake et al. (1997) for the photospheres of α Cen AB.
[2] This work.
[3] Mewe et al. (1998).
[4] Feldman et al. (1992).

Table 2. Comparison of SAX and ASCA observations[1]

Instr.	EM_1	T_1	EM_2	T_2	L_X	χ^2	d.o.f.
SAX	15	0.088	2.4	0.52	3.5[2]	9.0	10
ASCA	–	–	5.3	0.27	1.2	20.0	30
ASCA	4.3	0.081	5.3	0.27	2.7[3]	20.7	28

[1] EM in 10^{49} cm^{-3}, T in keV and L_X in 10^{27} erg/s in the 0.1-2.4 keV band.
[2] 80% from the 0.088 keV component.
[3] 56% from the 0.081 kev component.

the result of Sect. 4.1. The fit does not require any other significant DEM component beyond about 1 keV up to 10 keV. The result obtained with the Gauss fitting method is confirmed by a genetic algorithm (χ^2 = 11) which shows that the same two components found by the Gauss method are dominant and other components are either small or have large errors (thin solid line in Fig. 2).

5. Discussion

5.1. Temperature structure and X-ray luminosity compared to other observations

Similar to the ASCA observations (Paper II) the SAX observations do not require any hot ($\gtrsim$ 1 keV) component as would be required by fitting the SW "continuum" of the EUVE spectrum (cf. Paper I and also discussion in Paper II). Both 2-T fitting with δ functions and DEM fitting reveal a two-temperature structure with a soft (0.1 keV) and a somewhat harder (0.5 keV) temperature component. The soft component is comparable to that found by ROSAT and EUVE while the 2nd component is comparable to that found by EINSTEIN, EUVE, and ASCA (cf. Paper II, Sect. 6.1.). The strength of SAX is that it combines the soft and the hard regions.

To illustrate the problems to reconcile results from different instruments with different passbands we compare in more detail the SAX results to those of ASCA (cf. Table 1). If we fold the best-fit 1-T ASCA model ($T = 0.27$ keV, EM = 5.3 10^{49} cm^{-3}, cf. Paper II) with the derived ASCA abundances (see Sect. 5.2.) through the LECS response function we find that the "right lobe" of the LECS spectrum above 0.5 keV (cf. Fig. 1) is reasonably fitted but the "left lobe" below 0.3 keV is not. Adding a second component to the ASCA model with the first component fixed we are able to fit approximately also the left part of the LECS spectrum with a soft component (EM_2 = 4.3 10^{49} cm^{-3}, T_2 = 0.081 keV, χ^2 = 51) to which the ASCA instrument is essentially blind. Adding this component to the best-fit 1-T ASCA model indeed does not significantly change the minimum χ^2 for the ASCA observations (χ^2 increases from 20.0 for the 1-T model to only 20.7 for the 2-T model).

A comparison of the X-ray luminosities L_X (in 10^{27} erg/s) in the 0.1–2.4 keV band (cf. Table 1) yields 2.8 (T = 0.088 keV) and 0.7 (0.52 keV) for SAX and 1.2 (0.27 keV) for ASCA, while the additional soft component (0.081 keV) hardly seen by ASCA would give a luminosity of 1.5. Taking into account this soft flux the luminosities from the SAX and ASCA observations would be compatible, but we notice that intrinsic source variability can cause differences in the measured L_X of a factor of two or more on a timescale of ≤ 1 year (cf. Paper II).

5.2. Abundances

The α Cen system appears to be slightly (10%) older (age 5-6 Gyr) and of somewhat higher metallicity than the Sun (e.g., Lydon et al. 1993, Furenlid and Meylan 1990, Smith et al. 1986). The photospheric Fe abundance is well established, at [Fe/H] = 0.2, i.e. a value $\simeq 50\%$ higher than the solar photospheric Fe abundance (Chmielewski et al. 1992 and references therein). Claims about possible non-solar abundance ratios for various elements (including Mg and Si) have appeared in the literature, but, as discussed in detail in Drake et al. (1997), the more recent analyses appear to converge to a general enhancement of photospheric elemental abundance [X/H] = 0.2.

The best-fit value of the coronal Fe abundance (0.67±0.29) is slightly subsolar photospheric relative to the AG89 photospheric value or solar (0.95±0.41) relative to the GSN92 value (see Sect. 4.1.). For a number of young or intermediate-age solar analogs whose coronae have been observed with ASCA Güdel et al. (1997a,b) found that the coronal abundances were consistent with solar photospheric values, except for Mg which was twice overabundant. The coronal abundance ratios for Mg/Fe and Si/Fe derived for α Cen from our SAX observations are

consistent (within $\gtrsim 1\sigma$) both with the corresponding solar (and stellar) photospheric values and the solar coronal values (cf. Table 1). We can, therefore, not discriminate between photospheric values and the often observed tendency for coronal abundances to follow the so-called FIP effect (i.e., a relative overabundance of elements with low first ionization potential [FIP] and a relative underabundance of elements with high FIP; cf. Paper II). The O/Fe ratio is unusually high (O is a high-FIP element!), although we should note that the uncertainties are large.

There is a good agreement between the SAX Fe abundance of 0.67 ± 0.29 (Table 1) and that (0.77 ± 0.30) inferred from the the ASCA spectrum (cf. Paper II) which has a comparable number of counts (2827 cts vs. 2225 cts for SAX). The abundance determination with SAX profits from the well-defined continuum present at energies between 0.3–0.6 keV. About half of the total counts is in the form of line emission concentrated in the energy intervals 0.16–0.27 keV (100% line emission) and 0.56–1.02 keV (90% line emission), the remaining energy regions being practically dominated by pure continuum.

There is at the moment no satisfactory explanation for the different abundances derived from different observations, and for a discussion of various possible effects which may influence the determination of abundances we refer to Paper II.

The elemental abundances derived from EUVE, ASCA, and SAX may show some indications for a possible FIP effect as inferred from studies of the Sun (Feldman 1992, Feldman et al. 1992). However, in order to better constrain the absolute abundances relative to hydrogen a much better spectral resolution and S/N ratio such as can be achieved by AXAF and XMM is required.

5.3. DEM modeling and flare heating

Most of the sharpness of the reconstructed DEMs is undoubtedly introduced by the finite signal-to-noise ratio of the spectra and their finite spectral resolution combined with some bias inherent in the spectral DEM inversion techniques. In comparison, the solar DEM is certainly much broader, typically extending from about 0.1 to 0.5 keV (e.g., Watanabe et al. 1995). Therefore, we believe that the interval between the two DEM peaks is in actuality not fully devoid of plasma but that any addition of plasma to the model in that energy range would not improve the fit. Nevertheless, the emission measure distribution is surprisingly reminiscent of the key structure of the solar DEM. In solar active regions, the main contribution to the DEM stems from $\sim 0.4-0.5$ keV plasma while the quiet Sun defines a broad DEM around 0.1–0.3 keV (Watanabe et al. 1995). Peres et al. (1998) derived the average (active) solar DEM from full-Sun YOHKOH images. They simulated a "solar ROSAT" spectrum by folding the calculated emission through the ROSAT response for an appropriate exposure time. Spectral fits to this synthetic solar spectrum were satisfactory when assuming two plasma components, with temperatures of 0.13 keV and 0.44 keV, respectively, and an emission measure ratio of $\sim$12:1 (Peres et al. 1998). These values are very similar to ours of α Cen. This comparison actually suggests that we have observed α Cen during a time when it showed significant coverage by active regions.

In the solar case, the hot component relates to a hump in the solar DEM around 0.4–0.5 keV ascribed to the presence of active regions and indeed to the presence of microflaring as suggested by the variability in the "hot" S XV line (Watanabe et al. 1995). In somewhat more active solar-analog stars, this hot, separate hump becomes more prominent and is indeed compatible with time-averaged DEMs of larger solar flares (Güdel et al. 1997b). A model of stochastic flare heating predicts this two-T structure based on simple hydrodynamic properties of flares (Güdel 1997). In this framework, the hotter plasma found in α Cen points at a possible contribution of flares to the overall hot coronal plasma, a hypothesis that has gained new momentum in the light of recent SOHO results (e.g., Brekke et al. 1997). Observations like the present one may therefore give some new insights into topics of the "solar-stellar connection".

Acknowledgements. Part of this work was made possible by the support of the Space Research Organization of the Netherlands (SRON). MG acknowledges the hospitality of SRON during his visits. We thank Dr. Carole Jordan for some useful comments.

References

Anders E., Grevesse N., 1989, Geochimica et Cosmochimica Acta 53, 197 (AG89)
Arnaud M., Raymond J., 1992, ApJ 398, 394
Arnaud M., Rothenflug R., 1985, A&AS 60, 425
Boella G., Chiapetti L., Conti G. et al., 1997, A&AS 122, 327
Brekke P., Hassler D. M., Wilhelm K., 1997, Solar Phys. 175, 349
Chmielewski Y., Friel E., Cayrel de Strobel G., Bentolila C., 1992, A&A 263, 219
Drake J.J., Laming J.M., Widing K.G., 1997, ApJ 478, 403
Favata F., Maggio A., Peres, G., Sciortino, S., 1998, in: Bookbinder, J.A., Donahue, R.A. (eds.), Proc. 10th Cambridge Workshop on Cool Stars, Stellar Systems and the Sun, ASP Conference Series, San Francisco, in press
Feldman U., 1992, Phys. Scr. 46, 202
Feldman U., Mandelbaum P., Seely J.F., Doschek G.A., Gursky H., 1992, ApJS 81, 387
Flannery B.P., Ayres T.R., 1978, ApJ 221, 175
Furenlid I., Meylan T., 1990, ApJ 350, 827
Grevesse N., Noels A., Sauval A.J., 1992, in Coronal Streamers, Coronal Loops and Coronal and Solar Wind Composition, ESA SP-348, p. 305
Güdel M., 1997, ApJ 480, L121
Güdel M., Guinan E. F., Mewe R., Kaastra J. S., Skinner S. L., 1997a, ApJ 479, 416
Güdel M., Guinan E. F., Skinner S. L., 1997b, ApJ 483, 947
Kaastra J.S., Mewe R., 1993, Legacy, 3, 16
Kaastra J.S., Mewe R., Nieuwenhuijzen, H., 1996a, in: Yamashita K., Watanabe T. (eds.), UV and X-ray Spectroscopy of Astrophysical and Laboratory Plasmas, Universal Academy Press, Inc., Tokyo, p. 411
Kaastra J.S., Mewe R., Liedahl D.A. et al., 1996b, A&A 314, 547
Liedahl D.A., Osterheld A.L., Goldstein W.H., 1995, ApJ 438, L115
Lydon T.S., Fox P.A., Sofia S., 1993, ApJ 413, 390
Mewe R., Gronenschild E.H.B.M., van den Oord G.H.J., 1985, A&AS 62, 197

Mewe R. Lemen J.R., van den Oord G.H.J., 1986, A&AS 65, 511
Mewe R., Kaastra J.S., Schrijver C.J. et al., 1995a, A&A 296, 477
Mewe R., Kaastra J.S., Liedahl D.A., 1995b, Legacy 6, 16 (Paper I)
Mewe R., Kaastra J.S., White S.M., Pallavicini R., 1996a, A&A 315, 170
Mewe R., van den Oord G.H.J., Schrijver C.J., Kaastra J.S., 1996b, in: Bowyer S., Malina R.F. (eds.), Astrophysics in the Extreme Ultraviolet, Kluwer Acad. Publ., Dordrecht-Holland, p. 553
Mewe R., Drake S.A., Kaastra J.S. et al., 1998, A&A, in press (Paper II)
Morrison R., McCammon D., 1983, ApJ 270, 119
Parmar A.N., Martin D.D.E., Bavdaz M. et al., 1997, A&AS 122, 309
Peres G., Orlando S., Reale F., Rosner R., Hudson H., 1998, in T. Watanabe, T. Kosugi, A. C. Sterling, Observational Plasma Astrophysics: Five Years of YOHKOH and Beyond, Kluwer Academic Publ., in press
Smith G., Edvardsson B., Frisk U., 1986, A&A 165, 126
Watanabe T., Hara H., Shimizu T. et al., 1995, Solar Phys. 157, 169